

Magnetic Interactions in Phenyl-Bridged Nitroxide Diradicals: Conformational Effects by Multireference and Broken Symmetry DFT Approaches[†]

Vincenzo Barone,^{*,‡} Ivo Cacelli,[§] Paola Cimino,^{||} Alessandro Ferretti,[⊥] Susanna Monti,[⊥] and Giacomo Prampolini[#]

Scuola Normale Superiore, Piazza dei Cavalieri, I-56126 Pisa, Italy, Dipartimento di Chimica e Chimica Industriale, Università di Pisa, Via Risorgimento 35, 56126 Pisa, Italy, Dipartimento di Scienze Farmaceutiche, Università degli Studi di Salerno, Via Ponte Don Melillo, 84084 Fisciano (SA), Italy, Istituto per i Processi Chimico-Fisici del CNR, Area della Ricerca, Via G. Moruzzi 1, I-56122 Pisa, Italy, and Dipartimento di Chimica "Paolo Corradini", Università di Napoli Federico II, Via Cintia—Complesso Monte S. Angelo, 80126 Napoli, Italy

Received: June 6, 2009; Revised Manuscript Received: July 9, 2009

In the present paper we report the key results of a comprehensive computational study aimed at investigating the dependence of the singlet–triplet energy gap in phenyl-bridged bis-nitroxide diradicals, on the basis set and on soft structural parameters like torsion and pyramidalization. We have compared the BS-DFT technique with the post-Hartree–Fock DDCI2 multireference approach. With this latter method we have also studied the different role that σ and π core and virtual orbitals have in the resulting singlet–triplet energy gap. The results obtained represent one step forward in the definition of a protocol for an efficient and reliable computation of spin–spin coupling in diradical systems.

Introduction

Spin labeling has become in the past years one of the most useful techniques for investigating structure and dynamical behavior of complex systems related to both technological and biological fields. Use of this technique rests on the availability of reliable magnetostructural relationships involving both local (hyperfine and \mathbf{g} tensors) and long-range (J coupling and zero-field splitting) effects. This has stimulated a wealth of investigations aimed at developing, validating, and applying effective approaches to compute reliable values for these properties with no prohibitive computational costs. Methods rooted into the density functional theory have naturally emerged as the most effective tools coupling reliability and computational feasibility for the computation and analysis of local effects. As a matter of fact, hybrid functionals coupled to purposely tailored basis sets are starting to deliver results of quantitative accuracy for hyperfine and \mathbf{g} tensor of most radicals. The situation is more involved for the J coupling, which according to the Heisenberg Hamiltonian corresponds for diradicals to the singlet–triplet energy gap,¹ since only multireference post-Hartree–Fock approaches are able to deal rigorously with low-spin open-shell configurations. Although the broken-symmetry route has allowed interesting results to be obtained in a number of cases, its formal rigor is questionable, and, more importantly, it does not allow any analysis of effects related to electron density differences between different multiplet components. On the other hand, brute force multireference computations are out of question for the large magnetic systems of current chemical interest and perturbative approaches are ill adapted to this problem. A more

promising route is offered by the so-called difference dedicated configuration interaction (DDCI) approach in which classes of configurations affecting the energy difference between multiplet components are a priori selected and treated by a variational approach. Although this wise selection allows a strong reduction of the variational space, it is not sufficient whenever large magnetic systems are coupled by delocalized bridges. In a series of recent studies we have started the development of a general computational procedure in which molecular orbitals are localized, “external” ones (i.e., outside the localized magnetic moieties and the connecting bridge) are discarded, and virtual active orbitals are further reduced by placing suitable charges on the magnetic fragments (NO moieties in our case). The resulting MVO-frag approach has given promising results, but requires further testing and generalization in a number of connections. First, it is necessary to investigate basis set effects, which have not been analyzed in a systematic way for J couplings. Next, the respective role of σ and π electrons must be investigated, with the aim of further reducing in a systematic way the number of configurations treated at the variational level. From a different point of view, it is also interesting to analyze the performances of hybrid density functionals in the broken symmetry framework, together with the role of low-energy geometry deformations (essentially pyramidalization of the nitrogen environment and torsions around the C–N bonds) in tuning the magnetic properties.

In the present paper we use the model system HNO– ϕ –ONH, which is small enough to be treated in a nearly exact way within the DDCI2 scheme, to investigate the effects on the isotropic spin–spin interaction J of the basis set and of the conformational changes (torsion and pyramidalization) which may occur in these systems due to the environment (solution, solid state, etc.), by broken-symmetry density functional and DDCI2 calculations. The different role of σ and π core and virtual orbitals will also be discussed through DDCI2 computations of reduced dimensionality.

[†] Part of the “Vincenzo Aquilanti Festschrift”.

* Corresponding author. E-mail: vincenzo.barone@sns.it.

[‡] Scuola Normale Superiore.

[§] Università di Pisa.

^{||} Università degli Studi di Salerno.

[⊥] Istituto per i Processi Chimico-Fisici del CNR.

[#] Università di Napoli Federico II.

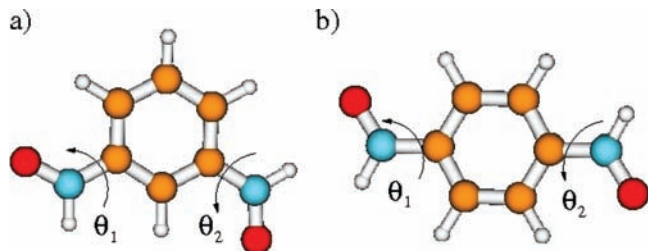


Figure 1. Phenyl-bridged nitroxide diradicals in their minimum energy conformation: (a) meta; (b) para. For both compounds, the torsional dihedral angles θ_1 and θ_2 are defined so that their optimized value corresponds to 180° and 0° , respectively.

Method and Computational Details

It is well-known that the minimal description of the magnetic interaction in a diradical system can be given within the 4-dimensional configurational space, obtained placing the two unpaired electrons in two nearly degenerate molecular orbitals ϕ_g and ϕ_u or, in a localized picture, in two orbitals localized on each magnetic site φ_a and φ_b (obtained by a unitary transformation of ϕ_g and ϕ_u). In weakly coupled systems both singlet and triplet states are essentially made by the two nonionic configurations, while in the lowest singlet the weight of the ionic configurations, those where the two electrons are in the same localized orbital, grows with the charge delocalization (or hopping).^{2–4} Such a minimal space alone is not sufficient for a quantitative description of the observed singlet–triplet energy gap, and extensive studies^{4–10} have shown that the contribution of excited configurations involving different core and virtual orbitals is significant for both metallic and organic systems.

In previous articles^{8,9} we have found that the DDCI2 scheme⁴ is sufficient to account for most of correlation and polarization effects in the ST energy gap, defined as $\Delta E_{TS} = E_T - E_S$, in benzene-bridged bis-nitroxides. Considering a further increase of the CI space by adding the configurations pertaining to the full DDCI scheme⁴ is found to contribute for the 10–15% maximum to the gap, and we have then decided to postpone a detailed investigation of the various contributions in DDCI focusing therefore here on the DDCI2 alone.

Since in this article we want to investigate the different factors influencing the spin–spin coupling in the rather small test cases of meta and para phenyl-bridged bis-nitroxide diradicals (Figure 1), we do not exploit the advantages of the modified virtual orbitals (MVO) approach presented and discussed in our previous work of ref 10, and we will then consider the complete orbital space.

For the meta and para bis-nitroxide species we have taken the geometry optimized at the DFT-UB3LYP level (cc-pvdz basis set; Gaussian03 package¹¹) in their high spin state.

The effects of change of basis have been studied using these reference geometries (Figure 1).

The torsional potential curves were obtained by optimizing all internal coordinates except the considered dihedrals θ_1 and θ_2 , as well as the pyramidalization angle ψ (see Figure 1 and Figure 2), which was initially constrained to 180° . In the computation of local minima, the constraint on ψ was eventually relaxed.

The canonical molecular orbitals were obtained by a ROHF calculation for the triplet state with the same basis set, using the GAMESS code.¹² The separation of σ and π orbitals in the planar systems was performed using the QUIOLA program coded by the authors, which interfaces the GAMESS output files with the routine for the transformation of the integrals from

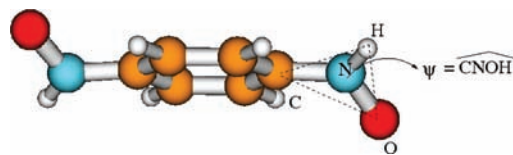


Figure 2. Definition of the pyramidalization angle ψ in the para phenyl-bridged nitroxide diradical with $\theta_1 = 45^\circ$ and $\theta_2 = 135^\circ$. The same ψ definition has been adopted for the meta compound.

TABLE 1: Singlet–Triplet Energy Splitting ΔE_{TS} (cm^{-1}) for the Para and Meta Phenyl Bridged Bis-Nitroxide Diradicals Computed with Several Basis Sets within the DDCI2 Scheme^a

basis	no. of MOs	DDCI2		DFT	
		para	meta	para	meta
6-311+G(d,p)	256	1942	−553	2165	−655
6-311+G(d)	238	1984	−565	2194	−667
6-311G(d)	198	1854	−541	2100	−651

^a In the second column the number of molecular orbitals of each employed basis set is reported. DFT values, reported for comparison, have been computed according to ref 23. All values have been computed on the planar minimum energy conformations displayed in Figure 1.

the atomic to the molecular basis set.⁸ The CI calculations were performed using the CIPSI program:^{13–15} all 1s core orbitals are kept inactive with occupation number 2 in all configurations.

In the DFT framework, the values of the magnetic exchange coupling constant term (J) have been calculated from differences between triplet and singlet energies by the so-called broken-symmetry (BS) approach.^{16–20} The physical description of magnetic coupling is based on the use of the following Hamiltonian,^{21,22} for two interacting particles with total spin angular momenta S_a and S_b : $\hat{H} = -2J\hat{S}_a\hat{S}_b$ (the chosen sign convention is that positive J corresponds to ferromagnetic coupling). The BS approach makes use of a description of the low spin state in an unrestricted, or spin polarized, formalism. Thus, $J = -(E_{HS} - E_{BS})/S_{\text{max}}^2$, where E_{HS} = energy of the high spin state (triplet), E_{BS} = energy of the broken symmetry singlet and S_{max} = spin of the triplet state. The Gaussian03¹¹ software has been used for the geometry optimization and for the DFT-BS calculations.

Results and Discussion

(i) Basis Set. Let us start by discussing the role of the basis set on the singlet–triplet energy gap. In order to calibrate an appropriate basis set, to be used in the DDCI scheme for the calculation of the triplet–singlet energy splitting for organic biradicals, a first set of calculations was performed on the para and meta species, in their minimum energy planar conformation. In Table 1 the resulting DDCI2 values are reported for both compounds, together with the values obtained by applying the DFT broken symmetry scheme.

It is quite apparent that diffuse functions (6-311+G(d) basis set) on heavy atoms and polarization functions on hydrogen atoms do not change the energy gap estimate in a substantial way, the relative error vs the largest basis set being $\sim 4\%$ and 2% , for the para and the meta compounds, respectively. Moreover the ΔE_{TS} value does not change in a monotonic way with the increase of the number of molecular orbitals (reported in the second column), neither in the para nor in the meta species. DFT computations enforce this conclusion, since the basis set dependence of broken symmetry results is, not surprisingly, even less pronounced.

TABLE 2: Singlet–Triplet Energy Splitting ΔE_{TS} (cm^{-1}) for the Para and Meta Phenyl Bridged Bis-Nitroxide Diradicals in the $\theta_1 = 45^\circ$ and $\theta_2 = 135^\circ$ Conformation^a

basis	DDCI2	
	para	meta
6-311+G(d,p)	576	-177
6-311+G(d)	589	-181
6-311G(d)	576	-173

^a All values have been computed within the DDCI2 scheme, with several basis sets, making use of the whole set of molecular orbitals.

TABLE 3: Contribution of σ and π Orbitals to the Computed Singlet–Triplet Energy Gap ($E_T - E_S$)^a

excitations cut	Ndet	$E_T - E_S$ (cm^{-1})	
		para	meta
$\sigma \rightarrow \sigma^*$	47804	1559.4	-589.2
$\pi \rightarrow \pi^*$	71254	965.9	-54.5
$\pi \rightarrow \sigma^*$	67004	1853.8	-496.0
$\sigma \rightarrow \pi^*$	64804	1853.8	-559.6
$\pi \rightarrow \sigma^*$	58404	1853.6	-521.4
$\sigma \rightarrow \pi^*$			
$\pi \rightarrow \sigma^*$	32804	1559.1	-615.0
$\sigma \rightarrow \pi^*$			
$\sigma \rightarrow \sigma^*$			
$\pi \rightarrow \sigma^*$	56254	965.7	-76.6
$\sigma \rightarrow \pi^*$			
$\pi \rightarrow \pi^*$			
$\pi \rightarrow \sigma^*$	30654	658.9	-91.3
$\sigma \rightarrow \pi^*$			
$\pi \rightarrow \pi^*$			
$\sigma \rightarrow \sigma^*$			
mag $\rightarrow \pi^*$			
$\pi \rightarrow \sigma^*$	53975	1352.9	-481.8
$\pi \rightarrow \sigma^*$	45375	1352.8	-495.0
$\sigma \rightarrow \pi^*$			
mag $\rightarrow \pi^*, \sigma^*$			
$\pi \rightarrow \sigma^*$	37079	1332.7	-482.9
$\pi \rightarrow \sigma^*$	28479	1332.6	-496.7
$\sigma \rightarrow \pi^*$			
mag $\rightarrow \sigma^*$			
$\pi \rightarrow \sigma^*$	39100	1831.6	-495.2
$\pi \rightarrow \sigma^*$	30500	1831.4	-520.9
$\sigma \rightarrow \pi^*$			
complete DDCI2 space	73404	1853.9	-534.4

^a The classes of excitation cut out from the complete DDCI2 space (last row) are given in first column, and the corresponding dimension of the CI space is in the second column; “mag” indicates both magnetic orbitals, e.g. those with one unpaired electron each.

As larger, but technologically more relevant, organic biradicals are experimentally found²⁴ in nonplanar conformations, the same basis set calibration was attempted in the $\theta_1 = 45^\circ$ and $\theta_2 = 135^\circ$ conformation of the two bis-nitroxide diradicals.

From the results reported in Table 2, it appears that the smaller basis set is even more reliable than for the planar conformations, the computed 6-311G(d) ΔE_{TS} values being almost coincident with those obtained with the larger 6-311+G(d,p) basis set.

In light of these results all DDCI2 calculations that follow were performed with the 6-311G(d) basis set.

(ii) Analysis of the σ/π Contribution for Planar Systems.

Planar conformations of the para and meta species allow an exact separation and analysis of the contribution of σ and π orbitals to the ST gap. The two radicals are taken in the most stable conformation with coplanar HNO fragments and phenyl bridge (with $\theta_1 = 180$ and $\theta_2 = 0$ in Figure 1).

The results of DDCI2 calculations performed considering the complete orbital space (198 orbitals for the 6-311G(d) basis

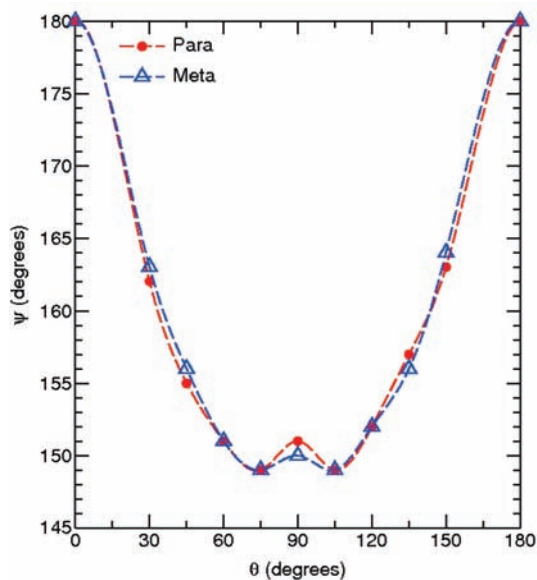


Figure 3. Pyramidalization angle ψ (see Figure 2) as a function of the torsional displacement $\theta = \theta_1 = 180^\circ - \theta_2$. Similar results were obtained for right and left pyramidalization angles. Geometry optimizations were performed at the B3LYP//cc-pvDz level on the triplet state of each compound.

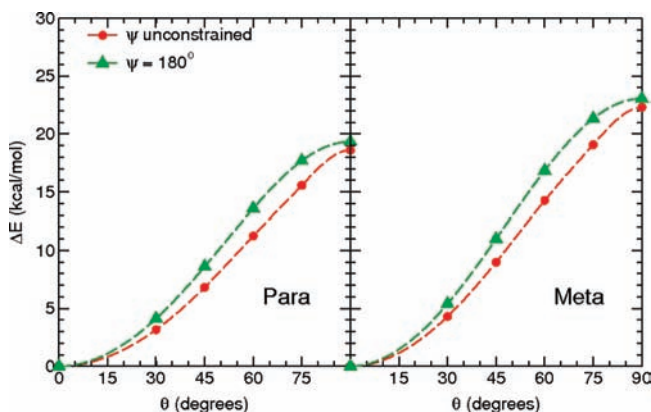


Figure 4. Conformational torsional energy of the triplet state as a function of the torsional displacement θ , corresponding, for both compounds, to a conformation with $\theta_1 = \theta$ and $\theta_2 = 180^\circ - \theta$ at the B3LYP//cc-pvDz level. The unconstrained results (circles) are obtained by relaxing all the internal coordinates but the θ displacement whereas in the other curve (triangles) ψ is fixed to 180° .

with the frozen 1s cores of C, N, and O atoms) but with various sets of configurations are reported in Table 3, for both para and meta species. The difference among the sets is that the configurations listed in the first column of Table 3 have been cut out from the full DDCI2 space. The reference values obtained for the complete DDCI2 space are also reported for comparison.

The first four rows of the Table clearly show the importance of $\pi \rightarrow \pi^*$ and $\sigma \rightarrow \sigma^*$ excited configurations. In fact, in both cases the gap results are too different from the reference values: too small for the para and too negative or too large for the meta. In particular, in the case where $\pi \rightarrow \pi^*$ excitations are neglected, we may notice a very strong variation in the gap, although the number of the $\pi \rightarrow \pi^*$ configurations is rather small (the CI space decreases from 73404 to 71254 configurations). This result underlines the importance of such excited configurations. On the other hand, the cross excitations $\pi \rightarrow \sigma^*$ and $\sigma \rightarrow \pi^*$ play a negligible role on the ST gap, especially for the para species.

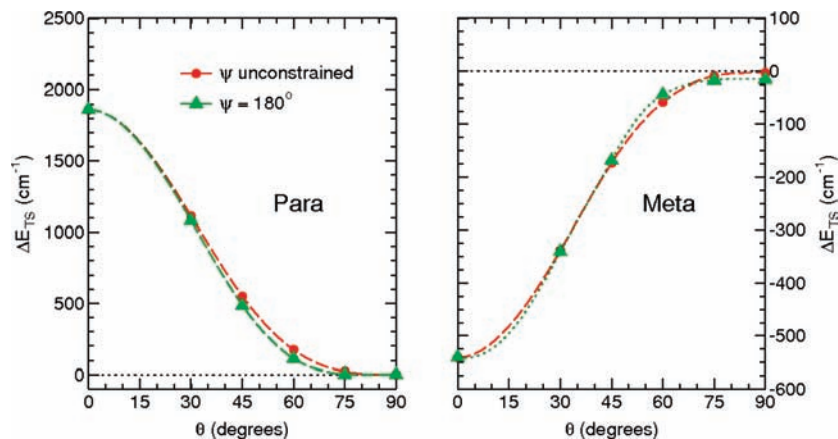


Figure 5. Singlet–triplet energy splitting ΔE_{TS} (cm^{-1}) curves for the para (a) and meta (b) phenyl bridged bis-nitronyl diradicals as a function of the torsional dihedral angle $\theta = \theta_1 = 180^\circ - \theta_2$. All values within the DDCI2 were computed with the 6-311G(d) basis set.

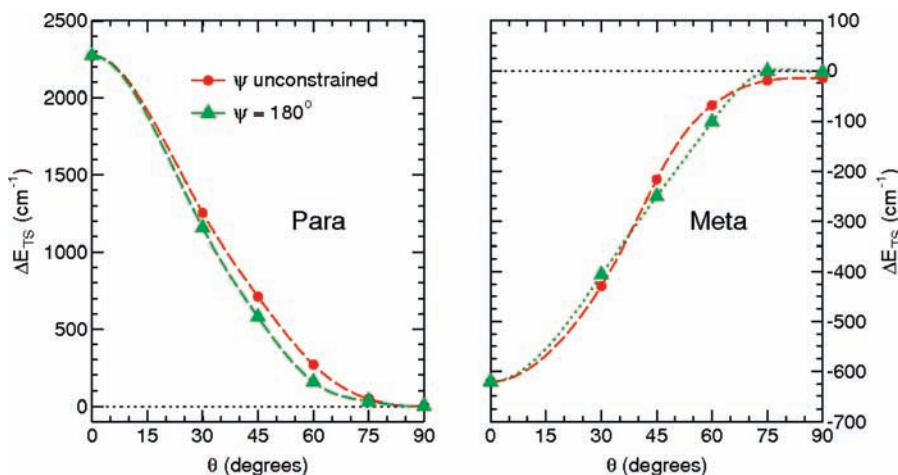


Figure 6. Singlet–triplet energy splitting ΔE_{TS} (cm^{-1}) curves for the para (a) and meta (b) phenyl bridged bis-nitronyl diradicals as a function of the torsional dihedral angle $\theta = \theta_1 = 180^\circ - \theta_2$. All values are computed with the DFT- broken symmetry scheme.

As expected the contemporary neglect of both $\pi \rightarrow \sigma^*$ and $\sigma \rightarrow \pi^*$ classes does not modify those conclusions but rather, in the case of the meta diradical where the neglect of $\pi \rightarrow \sigma^*$ subset caused a slight decrease in the ST gap while that of $\sigma \rightarrow \pi^*$ a slight increase, this results in a favorable error compensation (compare third and fourth rows with fifth row of Table 3). Any further cut involving double occupied-to-virtual excitation gives very bad results, as is clear from sixth, seventh and eighth rows of Table 1, where the neglect of $\pi \rightarrow \sigma^*$ and $\sigma \rightarrow \pi^*$ excitations is accompanied by that of $\sigma \rightarrow \sigma^*$ and $\pi \rightarrow \pi^*$ contributions taken either separately or together.

Once established that we must keep in the CI space the configurations arising from $\pi \rightarrow \pi^*$ and $\sigma \rightarrow \sigma^*$ excitation but we may neglect $\pi \rightarrow \sigma^*$ and $\sigma \rightarrow \pi^*$ contributions, we can analyze the role of different classes of excitations from the magnetic to the virtual orbitals. This is summarized in the three rows of Table 3 above that with the reference values, where, after disregarding $\pi \rightarrow \sigma^*$ or both $\pi \rightarrow \sigma^*$ and $\sigma \rightarrow \pi^*$ excitations, we further cut out the excitations from the two magnetic orbitals (e.g., those with formal single occupation) to π^* , σ^* , and $\pi^* + \sigma^*$ virtual orbitals. The results show that the $\text{mag} \rightarrow \pi^*$ (where mag indicates one of the two single occupied magnetic orbitals) excited configurations cannot be disregarded, whereas $\text{mag} \rightarrow \sigma^*$ excitations play a negligible role. As a matter of fact, for both para and meta diradicals neglect of $\text{mag} \rightarrow \sigma^*$, $\sigma \rightarrow \pi^*$, and $\pi \rightarrow \sigma^*$ excitations halves the dimension of the

CI space, worsening the computed ST energy gap by much less than 5% with respect to the reference values of the last row of the table.

(iii) Torsion/Pyramidalization Effects. In diradicals characterized by two magnetic moieties held together by a polyene or, as in the present case, an aromatic bridge, the isotropic spin–spin interaction strongly depends on the alignment of the magnetic orbitals with the π system of the bridge. It is therefore of interest to investigate how the molecular conformational changes affect the singlet and triplet state and the ST gap.

In both meta and para species, when each NO magnetic fragment is rotated out from the conformation in which it is coplanar with the ring, a pyramidalization at the N atom may occur, as a consequence of the loss of NO–ring electron delocalization. For the two magnetic moieties this occurs without any evident coupling, that is, for the two HNO–rings, the torsion/pyramidalization is independent one to each other.

In Figure 3, the dependence of the pyramidalization angle ψ (defined in Figure 2) on the torsion of the NO group, computed at the B3LYP/cc-pvDz level of theory, is reported. The torsional angle θ defines here a molecule with $\theta_1 = \theta$ and $\theta_2 = 180^\circ - \theta$ although, as discussed above, the two torsions are independent of each other. The reason for this choice is simply that many real bis-nitroxide diradicals, for which the species studied here may be seen as simplified models, are mostly characterized by an experimental equilibrium geometry of that kind with $\theta \neq 0$

and the dependence from θ alone, rather than a two-dimensional plot, is therefore of more practical interest.

We may notice from Figure 3 that the torsion/pyramidalization profile is roughly independent of the para or meta position of the two nitroxide fragments. ψ decreases (e.g., pyramidalization increases) up to a torsional angle of 75° , where a minimal value of $\psi = 149^\circ$ is reached and remains constant up to the conformation with the two NOs perpendicular to the ring plane (notice that the local maximum in Figure 3 at $\theta = 90^\circ$ is only 2° high).

The dependence of the torsional energy ΔE as a function of the θ displacement, computed at B3LYP//cc-pvDz level, is shown in Figure 4. The results for the two cases of relaxed geometry at each value of θ and of the diradical forced at zero pyramidalization at the nitrogen atoms are reported. The comparison of the two curves shows that the effect of pyramidalization, in both para and meta, is not very large and ranges between 1 and 3 kcal/mol.

(iv) Conformational Effects on the ST Energy Gap. We want now to discuss the effects of torsion/pyramidalization on the singlet–triplet energy gap. The dependence of ΔE_{TS} on the torsion θ , obtained by DDCI2 calculations using the 6-311G(d) basis and the complete resulting orbital space, is reported in Figure 5 for the para and the meta species, as well as for the two cases where the HNO–ring fragment is constrained or not in conformation without any pyramidalization ($\psi = 180^\circ$).

As expected the largest gap (in absolute value) occurs when the diradicals are planar and the delocalization of the magnetic orbitals on the ring is favored. At $\theta = 0$ we have then the largest antiferromagnetic interaction for the para and ferromagnetic interaction for the meta. In the two species the decrease of the absolute value of the gap with the torsion goes with the same slope and it is halved at $\sim 35^\circ$.

It is worthwhile noticing that the energy gap versus θ goes approximately as $\cos^2(\theta)$, which can be thought as the overlap between a localized magnetic orbital and a certain π benzene-like orbital belonging to the bridge. This behavior can be easily verified at $\theta = 45^\circ$ where the energy gap is about 1/4 of the maximum value for both compounds. This finding confirms that the magnetic coupling happens essentially through the bridge, as for $\theta = 45^\circ$ the two magnetic orbitals are orthogonal and a null splitting should be expected for direct through space interaction.

As far as the effects of pyramidalization on the energy splitting are concerned, it is apparent from the figure that they are small in both species; in the case of the meta species we may notice that the occurrence of pyramidalization gives rise to a small (13 cm^{-1}) ferromagnetic coupling even at torsion of 90° .

Since the configuration interaction methodology is computationally demanding, an alternative is provided by the DFT broken symmetry approach. This approach consists in performing unrestricted DFT calculations for low spin open-shell molecular systems in which α and β densities are localized on different atomic centers, which are referred to as BS calculations. The dependence of the magnetic coupling constant J on the torsion angles (ϑ_1 and ϑ_2) of the para and meta phenyl-bridged nitronyl diradicals is shown in Figure 6. The planar conformation corresponds to strong magnetic exchange interaction, whereas at 90° this interaction essentially vanishes (J is close to zero). As seen above for the CI data, we find that the J value (antiferromagnetic coupling) of the para species smoothly decreases with the increase of dihedral angle ϑ , whereas the J value (ferromagnetic coupling) for the meta species increases.

The general trends are in good agreement with the conclusions of the CI calculations, even if the DFT values are systematically larger (Figure 6).

Conclusions

The present paper is devoted to a comprehensive analysis of the tuning of the singlet–triplet energy gap in model nitroxide diradicals by basis set and by specific conformational changes, such as torsion and pyramidalization, which may occur in relation to specific environmental conditions (solution, solid state, etc.). For this study we have chosen phenyl-bridged bis-nitroxide diradicals for two reasons: first they are small enough to allow extensive and reliable calculations, and second the relative position of the two nitroxide units bearing the unpaired electrons with respect to the phenyl ring (para or meta) allows the contemporary study of closely related antiferromagnetic and ferromagnetic systems. We have compared the BS-DFT technique with the post-Hartree–Fock DDCI2 multireference approach. With this latter method we have also investigated the different role that σ and π core and virtual orbitals play in determining the singlet–triplet energy gap.

As far as the effect of the basis set is concerned, we have found that both BS-DFT and DDCI2 approaches are scarcely sensitive to the inclusion of diffuse functions on heavy atoms and polarization functions on hydrogen atoms. The torsion of the two HNO magnetic fragments with respect to the ring decreases the spin–spin coupling so that in nonplanar diradicals the quasi-degeneracy of singlet and triplet states increases independently from para or meta substitution. For the rotated species, pyramidalization at the nitrogen, which brings to more stable conformations, has an overall small effect on the singlet–triplet gap except at large torsions for the meta species, where it prevents the reach of a full singlet–triplet degeneracy.

Finally, for the planar systems where full σ/π separation is allowed, we have identified the contribution to the resulting gap of the various core and virtual orbitals and shown that we may more than halve the configurational space neglecting all $\text{mag} \rightarrow \sigma^*$, $\pi \rightarrow \sigma^*$ and $\sigma \rightarrow \pi^*$ excitations (where “mag” refers to the magnetic orbitals).

The present results represent, in our opinion, a further significant step toward the definition of a general computational protocol for an efficient and reliable computation of spin–spin coupling terms in diradical systems.

References and Notes

- (1) Kahn, O. *Molecular Magnetism*; VCH: New York, 1993.
- (2) Hay, P. J.; Thibault, J. C.; Hoffmann, R. *J. Am. Chem. Soc.* **1975**, *97*, 4884.
- (3) de Loth, P.; Cassoux, P.; Daudey, J. P.; Malrieu, J.-P. *J. Am. Chem. Soc.* **1981**, *103*, 4007.
- (4) Calzado, C. J.; Cabrero, J.; Malrieu, J.-P.; Caballol, R. *J. Chem. Phys.* **2002**, *116*, 2728.
- (5) Cabrero, J.; Ben Amor, N.; de Graaf, C.; Illas, F.; Caballol, R. *J. Phys. Chem. A* **2000**, *104*, 9983.
- (6) Calzado, C. J.; Cabrero, J.; Malrieu, J.-P.; Caballol, R. *J. Chem. Phys.* **2002**, *116*, 3985.
- (7) Moreira, I. d. P. R.; Illas, F. *Phys. Chem. Chem. Phys.* **2006**, *8*, 1645.
- (8) Barone, V.; Cacelli, I.; Ferretti, A.; Giralda, M. *J. Chem. Phys.* **2008**, *128*, 174303.
- (9) Barone, V.; Cacelli, I.; Ferretti, A. *J. Chem. Phys.* **2009**, *130*, 94306.
- (10) Barone, V.; Cacelli, I.; Ferretti, A.; Prampolini, G. *Phys. Chem. Chem. Phys.* **2009**, *11*, 3854.
- (11) Frisch, M. J.; et al. *Gaussian 03*, revision B.04; Gaussian Inc.: Pittsburgh, PA, 2003.
- (12) Schmidt, M. W.; Baldrige, K. K.; Boats, J. A.; Elbert, S. T.; Gordon, M. S.; Jensen, J. H.; Koseki, S.; Matsunaga, N.; Nguyen, K. A.; Su, S. J.; Windus, T. L.; Dupuis, M.; Montgomery, J. A. *J. Comput. Chem.* **1993**, *14*, 1347.

- (13) Huron, B.; Malrieu, J.-P.; Rancurel, P. *J. Chem. Phys.* **1973**, *58*, 5745.
- (14) Evangelisti, S.; Daudey, J. P.; Malrieu, J.-P. *Chem. Phys.* **1983**, *75*, 91.
- (15) Cimiraglia, R.; Persico, M. *J. Comput. Chem.* **1987**, *8*, 39.
- (16) Improta, R.; Kudin, K. N.; Scuseria, G. E.; Barone, V. *J. Am. Chem. Soc.* **2002**, *124*, 113.
- (17) Noodleman, L. *J. Chem. Phys.* **1981**, *74*, 5737.
- (18) Noodleman, L.; Baerends, E. J. *J. Am. Chem. Soc.* **1984**, *124*, 113.
- (19) Bencini, A.; Totti, F.; Daul, C.; Doclo, K.; Fantucci, P.; Barone, V. *Inorg. Chem.* **1997**, *36*, 5022.
- (20) Adamo, C.; Barone, V.; Bencini, A.; Broer, R.; Filatov, M.; Harrison, N. M.; Illas, F.; Malrieu, J. P.; Moreira, P. R. *J. Chem. Phys.* **2006**, *124*, 107101.
- (21) Heisenberg, W. *Z. Phys.* **1928**, *49*, 619.
- (22) Dirac, P. A. M. *The Principles of Quantum Mechanics*; Clarendon: Oxford, 1947.
- (23) Ali, M. E.; Datta, S. N. *J. Phys. Chem. A* **2006**, *110*, 2776.
- (24) Shultz, D. A.; Fico, R. M.; Lee, H.; Kampf, J. W.; Kirschbaum, K.; Pinkerton, A. A.; Boyle, P. D. *J. Am. Chem. Soc.* **2003**, *125*, 15426.

JP9053346